Tameh, E. K., Nix, A. R., & Beach, M. A. (1997). A 3-D integrated macro and microcellular propagation model, based on the use of photogrammetric terrain and building data. 1957 - 1961. 10.1109/VETEC.1997.605900

A 3-D INTEGRATED MACRO AND MICROCELLULAR PROPAGATION MODEL, BASED ON THE USE OF PHOTOGRAMMETRIC TERRAIN AND BUILDING DATA.

Eustace K. Tameh *Andrew R. Nix* *Mark A. Beach*
Centre for Communications Research, University of Bristol
Merchant Venturers Building, Woodland Road,
Bristol BS8 1UB, UK
Tel:+44 117 954 5169, Fax: +44 117 954 5201; Email: Tek.Tameh@bristol.ac.uk

Abstract: This paper describes a fully three-dimensional deterministic propagation model based on a radar cross-section analysis of terrain pixels and building walls. The model utilises a variable resolution terrain database as well as a buildings database to predict signal strength, time dispersion and fading information, in addition to providing spatial information (e.g. arrival angles) for the propagation channel. It considers scattering from illuminated terrain pixels and building walls as well as considering off-axis terrain and rooftop diffraction contributions.

The model can be particularly useful for integrating macrocells and microcells e.g. predicting interference in a microcell due to a nearby macrocell or vice versa. Signal strength predictions from the model show good agreement with narrowband measurements for a rural macrocell. The effects of buildings and foliage in the propagation channel are investigated, and reveal that large errors can result if these effects are ignored. The accuracy improvement of the 3-D analysis over the simpler 2-D approach is also demonstrated.

I. INTRODUCTION

In most environments, wave propagation from transmitter (Tx) to receiver (Rx) is not restricted to the vertical Tx-Rx plane but includes contributions from scattered fields off this plane [1,2]. The resulting multipath propagation leads to a time dispersion of the received signal. Some knowledge of this dispersion (or a suitable measure of it) is particularly important for evaluating the performance of digital communications systems [3]. Also, with the increasing use of smart antenna technology to improve system performance, there is a strong requirement for spatial information (e.g. arrival angles) for future mobile communications systems [4]. Clearly, conventional two-dimensional models which only consider propagation in the vertical Tx-Rx plane are inadequate for these purposes. This necessitates a three-dimensional approach to propagation modelling to obtain this channel information [3].

Even in urban areas where microcells and picocells predominate, these small cells exist alongside larger cells (radius > 1Km) and it is often necessary in network planning to determine the interference effects between one cell and the other (C/I). There is a need for fast and efficient prediction models which integrate propagation in macrocellular environments with some of the main features of propagation in microcells, particularly building scatter and rooftop diffraction. Whereas lateral or corner diffraction is the dominant diffraction mechanism for coverage within microcells (with base station antennas typically below rooftop level), wave propagation between microcells and macrocells mainly involves rooftop diffraction. Also, individual buildings can significantly affect propagation in built-up areas, particularly in the vicinity of the transmitter and receiver; as such some knowledge of the position, shape and size of each building is required [5].

In this paper we present a fully three-dimensional deterministic model which uses a 3-D raster database for buildings in addition to a variable resolution Digital Terrain Map (DTM). It considers scattering from terrain and building walls as well as diffraction over rooftops and terrain obstacles. The three-dimensional model is described in section II, while section III presents some of the predictions from the model and compares them with narrowband measurements carried out in the prediction area. The importance of buildings and foliage is investigated as is the accuracy improvement of the 3-D analysis compared to the more simple 2-D approach.

II. PROPAGATION MODEL

The model predicts signal strength, time dispersion (complex impulse response and delay spread), fast fading (Rician K factor) as well as arrival angles for all rays at the receiver. Predictions are made for single receivers points, multiple receiver points (random locations or locations along a specified route), as well as for specified areas (i.e. circular or rectangular grids).

A. INPUT DATA

The DTM contains raster terrain elevation data with 50m resolution and covers a 10Km x 10Km area. The elevation data has been commercially obtained by the use of aerial photography and photogrammetric techniques.

0-7803-3659-3/97 $10.00 ©1997 IEEE

The terrain is then modelled as a series of plane scattering surfaces, each plane uniquely identified in three-dimensional space by its centre point and normal vectors. However, planes which fall within built-up areas are further subdivided into 10m x 10m sub-pixels, giving rise to a variable resolution DTM.

A buildings database consisting of three-dimensional raster cells with 10m resolution is then superimposed on to the variable resolution DTM. Each isolated building is modelled as a solid polygon of a specified height, and contributes 5 scattering areas or pixels, corresponding to the walls and roof of the building. Fig. 1 illustrates the buildings on the variable resolution DTM.

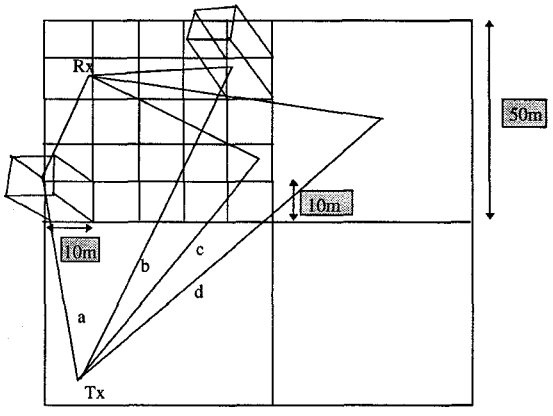

Fig. 1: 3D model showing buildings on DTM

This somewhat coarse representation of buildings is considered reasonable for the purposes described earlier, and is considered necessary to allow large terrain areas up to 10Km x 10Km to be modelled.

In addition to the DTM and buildings database, we use a clutter database which defines the ground cover for each terrain pixel. Each pixel belongs to one of 10 ground cover classes, each class having pre-defined surface roughness parameters (standard deviation of surface heights and correlation length [6]) and electrical properties (permittivity and conductivity). The initial values used for these parameters were obtained from the literature (e.g. [7]) but are intended to be tuned following validation measurements. For simplicity, all building walls are assumed to have the same composition (i.e. electrical properties and surface roughness parameters).

B. PATH LOSS CALCULATIONS

1) Scattered Paths

Each illuminated terrain pixel and building wall contributes a unique propagation path between the transmitter and receiver. Illumination is defined by:

$$0 < \vartheta_i, \vartheta_r < 90^0 \qquad (1)$$

where ϑ_i and ϑ_r are the incident and scattering angles between the normal to the pixel and the directions to the transmitter and receiver respectively. For pixels without line-of-sight (LOS) to transmitter and receiver, these angles are calculated from the closest diffraction edge to the pixel. Only first order scattering is considered in the current implementation of the model.

To determine diffraction losses, terrain profiles from the transmitter to each pixel, and from the pixel to the receiver, are reconstructed, taking into account the variable resolution nature of the database. Diffraction losses are then estimated using Fresnel's knife-edge diffraction equation, for up to two knife edges along the profile. Picquenard's diffraction construction ([8]) is used for multiple diffraction edges.

The power contributed by each scattering surface is obtained from the radar equation:

$$P_r = \frac{P_t G_t(\theta,\phi) G_r(\theta,\phi) \lambda^2 \sigma}{(4\pi)^3 R_t^2 R_r^2} L_d \qquad (2)$$

where:

- σ is the bistatic radar cross section of the surface
- P_t is the total transmitted power
- $G_t(\theta,\phi)$ and $G_r(\theta,\phi)$ are the transmitter and receiver antenna gains in the direction (θ,ϕ) respectively
- R_t and R_r are the distances from the pixel to the transmitter and receiver respectively and
- L_d is the total diffraction loss in the 2 path profiles.

Two approaches for the calculation of the bistatic radar cross-section , σ, have been investigated:

- the Kirchhoff and small perturbation method ([9]) and
- a modified form of the Lambertian emitter model (modified to take into account the effects of surface roughness) [10].

Both methods produced similar results but the latter was adopted due to the mathematical complexity of the Kirchhoff and small perturbation approach.

Lastly, the arrival angle for each ray is calculated, and the phase angle for the ray is then calculated from its path length.

2) Direct Path

Free space propagation is assumed in the direct path between the transmitter and receiver. In addition to the free space loss, the model can add diffraction losses for up to 5 diffractions, a loss due to inadequate Fresnel zone clearance, and losses due to the presence of foliage in the path. Foliage loss calculations are based on an empirical formula derived from measurements ([11]). These calculations make use of a vectorised database of hedgelines and tree locations.

C. EXTENSION OF VARIABLE RESOLUTION APPROACH FOR LARGE AREAS.

To increase computational speed when dealing with large areas, the variable resolution approach is extended

as follows. The prediction area is divided into three zones bounded by three confocal ellipses, with the transmitter and receiver at the foci. The inner, middle and outer zones have resolutions of 50m, 100m and 200m respectively. The size of the ellipses are specified prior to each run as part of the input parameters to the program. Buildings are only considered in the innermost zone as the effects of buildings are deemed to be most significant in the vicinity of the transmitter and receiver. Also, in the middle and innermost zones, scattered paths are only considered if at most two diffractions are encountered, but for the outer zone, only pixels with LOS to both transmitter and receiver are considered. It is believed (and results confirm) that there is no significant loss of accuracy as a result of this approach. This is because, in general (but not always) contributions to the received power from pixels decrease with increasing distance from the transmitter and receiver; as such we consider it reasonable to progressively decrease the terrain resolution (and thereby improve speed) for those pixels further away from the transmitter and receiver. This approach is illustrated in Fig. 2.

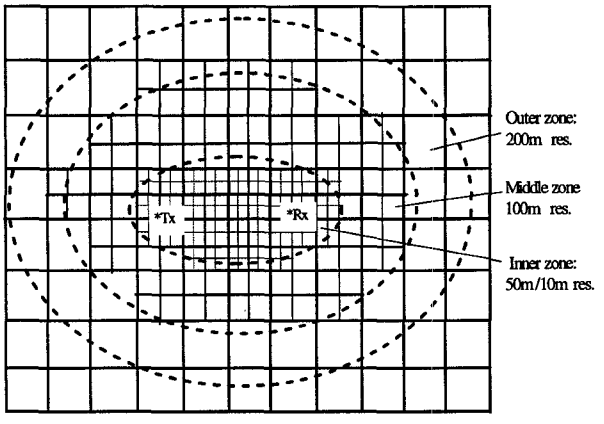

Fig. 2: Variable resolution approach for large areas.

This technique has the further advantage of allowing us to investigate the sensitivity of the measured and predicted results to the terrain resolution, by judiciously allocating the sizes of the ellipses. In addition, by varying the size of the innermost ellipse we can evaluate the effect or importance of buildings as a function of distance from the transmitter and receiver.

D. MODEL OUTPUT

The instantaneous received power is the phasor sum of all rays in the direct and scattered paths. The rms. delay spread and the Rician K factor for the channel are calculated from the complex impulse response. The model supports full 3-D antenna patterns and arbitrary 3D polarisation states.

Fig. 3a shows a sample output of the model. It illustrates the three-dimensional variable resolution database for a 1Km x 1Km slice of the available area, and shows the 10 strongest ray paths from the transmitter to the receiver (strength proportional to thickness of ray; - the program will find many hundreds of rays, however, for visualisation purposes, only the most significant are displayed). Fig. 3b then shows the resulting impulse response, while Fig. 3c shows the arrival angles at the receiver for the rays shown in impulse response. Fig. 3d illustrates the received power predicted for a specified route and shows the differences in prediction for the 2-D (vertical plane) and 3-D approaches. It also shows the effect on the signal strength of neglecting the effects of individual buildings (building scatter and rooftop diffraction) for a specified route.

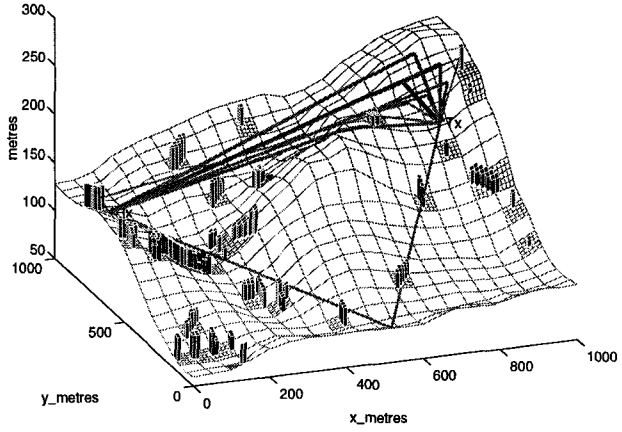

Fig. 3a: 1Km x 1Km map showing 10 strongest rays from Tx to Rx

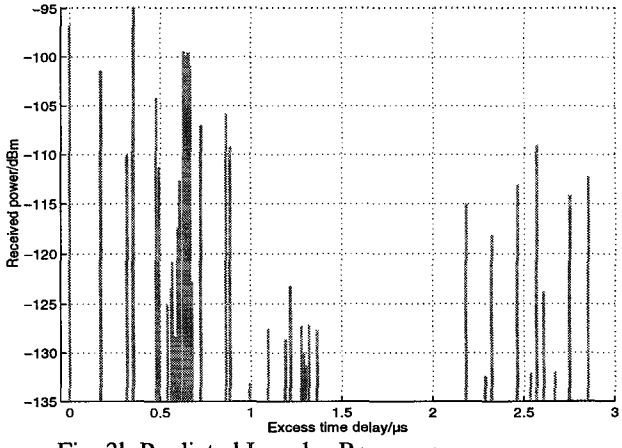

Fig. 3b:Predicted Impulse Response

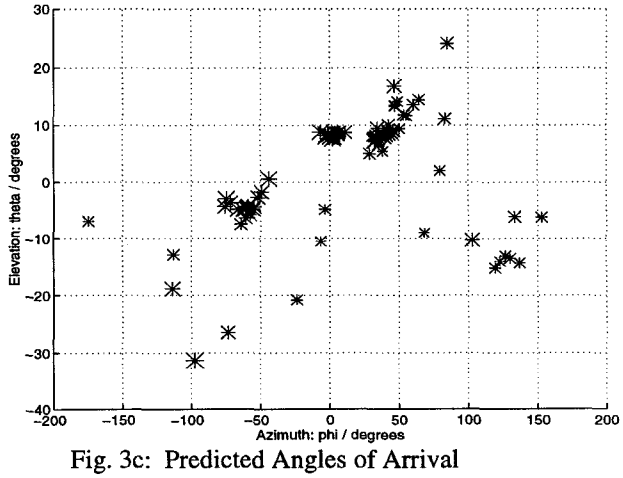

Fig. 3c: Predicted Angles of Arrival

$-90^0 <= \text{theta} <= 90^0$; theta = 0^0 along x-axis.
$-180^0 <= \text{phi} <= 180^0$;

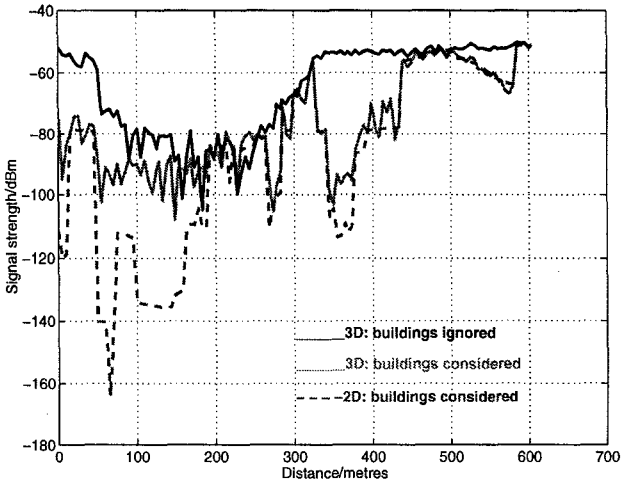

Fig.3d: Effect of buildings on power profile for route

From Fig. 3d the mean difference in signal level between the 3-D profile ignoring buildings, and the profile considering buildings is quite high - of the order of 15dB, as is the difference between the 2-D and the 3-D profiles (considering buildings).

III. MEASUREMENTS AND ANALYSIS

A. MEASUREMENTS

Narrowband measurements have been made in an urban and a rural macrocell, at 1823MHz. These measurements were aimed, not only at validating the developed model, but primarily at tuning the model parameters such as the electrical and surface roughness values for scattering off terrain and buildings, as well as the foliage attenuation calculation parameters. We present results for the rural area measurements, carried out in Dundry, a village on the outskirts of Bristol. Results for the urban area are being processed and will be presented at the conference.

Fig. 4 shows a contour map of the area, indicating the base station and measurement route locations.

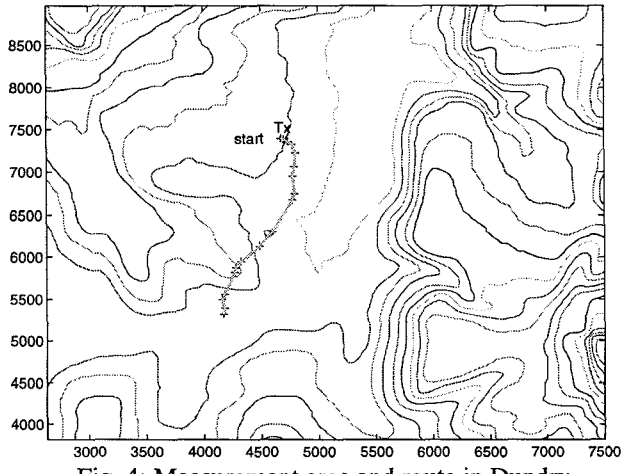

Fig. 4: Measurement area and route in Dundry

The measurements were made using a car field survey system (FSS), with the receiver antenna mounted on the roof of the car (1.5m high). The transmitter and receiver antennas were both dipoles, with the transmitter antenna mounted on a pump-up mast at a height of 10m. The total transmitted power (EIRP) was 33dBm.

Fig. 5 and Fig. 6 show the measurements for a vertically polarised and a horizontally polarised transmitter respectively, compared with the 3-D and 2D model predictions. Finally, the effects of neglecting foliage and buildings is demonstrated in Fig. 7.

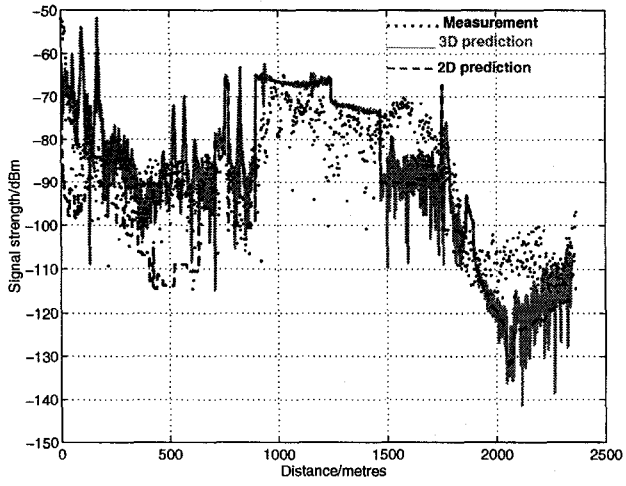

Fig. 5: Route profile for vertically polarised Transmitter.

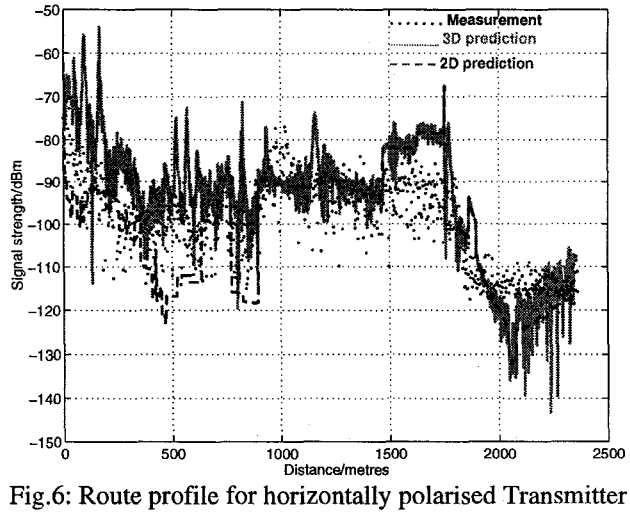

Fig.6: Route profile for horizontally polarised Transmitter

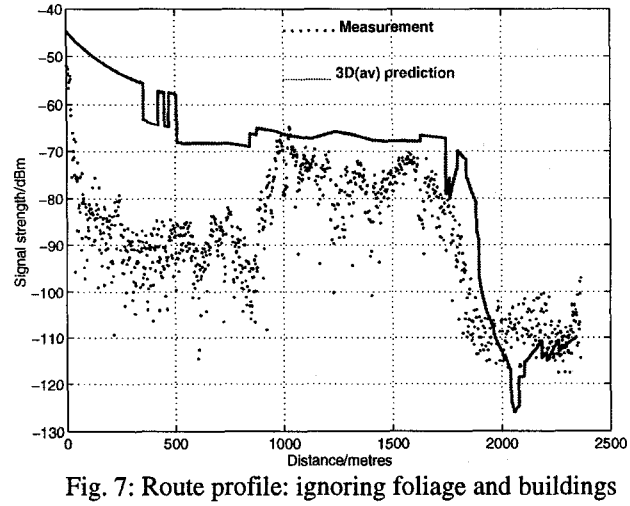

Fig. 7: Route profile: ignoring foliage and buildings

B. ANALYSIS

The primary aim of the measurements was to investigate and understand the importance of modelling foliage and buildings, and not just a validation exercise. The chosen route in Fig. 4 has hedges (about 3m-5m high and 2m thick) on both sides of the route, close to the starting point. This was considered useful for fine-tuning the foliage loss calculations in the model. Additionally, there were a few farmhouses close to the transmitter location, and along the measurement route.

The predictions made use of the ellipse-bounded zonal approach illustrated in Fig. 2, with the innermost ellipse enclosing all the buildings within a distance 500m greater than the direct distance from the transmitter to the receiver.

In general, good agreement is obtained for the 3-D approach, with an overall rms. error of 7.5dB for the vertically polarised transmitter (Fig. 5), and 8dB for the horizontally polarised transmitter (Fig. 6). The rms. error is slightly higher for the first half of the route due to inaccuracies in the foliage attenuation calculations. A more analytic approach (e.g. [12]) is being investigated to replace the current empirical one.

Fig. 5 and Fig. 6 clearly illustrate that even for a relatively flat area, a three-dimensional approach still produces more accurate results than simply considering the two-dimensional vertical cut from the transmitter to the receiver, in addition to providing extra channel information (time dispersion, fading, and spatial information). The rms. errors between the 2-D profiles and the measurements increase to 11.5dB for the vertically polarised transmitter (Fig. 5), and 10.5dB for the horizontally polarised transmitter (Fig. 6). The importance of considering foliage and buildings in the propagation path, especially in the vicinity of the transmitter and receiver is emphasised by Fig. 7. Attenuation values of up to 20dB are observed due to the presence of thick hedges and tree canopies, giving an overall rms. error of 18dB between the prediction and measurements (Fig. 7). This high error was due to the low height of the transmitter above the ground (10m) which allowed the direct path to the receiver to always be blocked by foliage.

IV. CONCLUSION

We have presented a three-dimensional propagation model based on a variable resolution terrain and buildings database. The model can integrate propagation in macrocellular and microcellular environments and as such is useful for interference calculations between macrocells and microcells. The model supports full off-axis roof-top and terrain diffraction, combined scattering from buildings and terrain features, and combinations of these, as well as foliage attenuation. Initial measurements in a rural macrocell have been presented and show good agreement with model predictions. We have shown that neglecting foliage and building effects can lead to rms. errors as high as 18dB. The accuracy improvement of the 3-D analysis over the 2-D approach has also been demonstrated., with an rms. error of 7.5dB obtained for the 3-D model considering foliage and building effects. A better characterisation of foliage attenuation is currently under investigation.

V. ACKNOWLEDGEMENT

Much of the work described in this paper was carried out under the Virtual University Research Initiative (VURI) and funded by British Telecommunication Research Laboratories at Martlesham, UK. The authors are also grateful to Prof. J. P. McGeehan of the Centre for Communications Research, Bristol, as well as other members of the Centre, for their help and suggestions regarding this work. We are particularly grateful to Dr. Steven Meade for his help in obtaining the results.

REFERENCES

[1] T. Kurner, D. Cichon, W. Wiesbeck, *Concepts and Results for 3D Digital Terrain-Based Wave Propagation Models: An Overview*, IEEE Trans. on Comm. vol. COMM-II, Sept. 1993, pp. 1002-12.

[2] Hermann Buhler, Ernst Bonek, Boris Nemsic, *Estimation of Heavy Time Dispersion for Mobile Radio Channels Using a Path Tracing Concept,* 43rd VTC, 1993, vol. 2, pp. 257-260.

[3] Bernard H. Fleury, Peter E. Leuthold, *Radiowave Propagation in Mobile Communications: An Overview of European Research*, IEEE Communications Magazine, Feb. 1996, pp.70-81.

[4] G. V. Tsoulos, M.A. Beach, S.C. Swales, *Adaptive Antennas for Third Generation DS-CDMA Cellular Systems*, 45th VTC, July 1995, Chicago, vol. 1, pp. 45-49.

[5] G. E. Athanasiadou, A. R. Nix, J. P. McGeehan, *A Ray-Tracing Algorithm for Microcellular Wideband Propagation Modelling,* VTC `95, Chicago, vol. 1, pp. 261-265.

[6] Beckmann, P. and A. Spizzichino, *The scattering of electromagnetic waves from rough surfaces*, Pergamon Press, 1963.

[7] M. Lebherz, W. Wiesbeck, W. Krank, *A versatile wave propagation model for the VHF/UHF range considering three-dimensional terrain,* IEEE Trans. Ant. and Prop. , vol. 40, pp 1121 - 1131, 1992.

[8] Picquenard, A., *Radio wave propagation*, Wiley, 1974.

[9] T. Ulaby, R. K. Moore, A. K. Fung, *Microwave Remote Sensing: Active and Passive, vol. II,* Reading, MA, Addison - Wesley, 1982.

[10] T. Brook, P.F. Driessen, R.L. Kirlin, *Propagation Measurements using Synthetic Aperture Radar Techniques*, 45th VTC, July 1995, Chicago, vol. 2, pp. 1633-37.

[11] M. Al-Nuaimi, A. Hammoudeh, *Theoretical and experimental study of attenuation and scatter of microwave signals by trees,* ICAP 93, No. 370, part II, pp 808-811.

[12] T. Tamir, *Radio wave propagation along mixed paths in forest environments*, IEEE Trans. on Ant. and Prop., vol.25, No. 4, 1977, pp 471-477.